Soils and Rocks
An International Journal of Geotechnical and Geoenvironmental Engineering
www.soilsandrocks.com
ISSN 1980-9743
ISSN-e 2675-5475

Microbially induced calcite precipitation (MICP) in a sandy soil for strength improvement and contaminant immobilization

Vinicius Luiz Pacheco[1], Cleomar Reginatto[1#], Antônio Thomé[1]

Article

Keywords
Biocementation
Inorganic contaminants
Sandy soil

Abstract

Microbially induced calcite precipitation (MICP) is a sustainable technology which utilizes biochemical processes, to produce calcium carbonate ($CaCO_3$) in the presence of Urea, calcium chloride ($CaCl_2$), and microorganisms. The application of the MICP process, via biostimulation of natural microorganisms, to a natural sandy soil that was contaminated in the laboratory with hexavalent chromium (Cr^{6+}) and cadmium (Cd^{2+}) was investigated. The improvement of the soil's geomechanical strength and the increase in its capacity to immobilize both contaminants were evaluated. An experimental program was carried out with bioreactors to evaluate the influence of three main parameters: Cr^{6+} (X1), Cd^{2+} (X2) and the volume of biocementation solution (X3). The experiment was carried out in the laboratory, with bioreactors, with 5cm of contaminated soil, 25 cm of uncontaminated soil and 10 cm for insertion of the biocementation solution. Monitoring of urease behavior indicated that initial concentrations of 20 mg.kg^{-1} and 40 mg.kg^{-1} for Cr^{6+} and Cd^{2+}, respectively, were not toxic to urea hydrolysis. Movement of contaminants occurred during the leaching of the biocementation solution, however, contaminant immobilization showed maximum values of 95.67% for Cd^{2+} and 87% for Cr^{6+}. The uniaxial compressive strength (UCS) test reached values between 114.84 and 917.43 kPa. This indicates that $CaCO_3$ precipitation occurs even in a toxic environment, immobilizing and promoting the biomineralization of contaminants. In conclusion, MICP could be a promising sustainable technique for application in contaminated soil.

1. Introduction

The increasing use of industrialized products generally ends up with several types of contaminants. Among these, metals have great attention for their toxicity, mobility, and permanence in contaminated sites. Residues containing hexavalent chromium (Cr^{6+}) and Cadmium (Cd^{2+}) are among the most toxic and recognized as human carcinogen (GracePavithra et al., 2019; Liu et al., 2018).

Several techniques can be used to remediate these contaminated areas, preventing the movement of contaminants, such as techniques for stabilizing and solidifying. In this sense, more efficient and sustainable techniques are sought to immobilize soil contaminants, as is the case of the microbially induced calcite precipitation (MICP) technique. (Song et al., 2022; Chen et al., 2023).

Biocementation, also named MICP, has been applied. Can be used in addition of conventional cement in mortar and concrete; and for the immobilization of toxic metals (Achal et al., 2009; Yang & Cheng; 2013; Al-Salloum et al., 2017; Gomez et al., 2017; Li et al., 2018; Mwandira et al., 2017; Liu et al., 2018).

Furthermore, the application of MICP extends to the remediation of cracks in structural materials and the stabilization of heavy metals in contaminated soils. For instance, Li et al. (2018) demonstrated the successful bio-consolidation of cracks in masonry cement mortars using Acinetobacter sp. SC4, a high-urease-producing bacterium isolated from a karst cave, which resulted in significant improvements in compressive strength and reduction in water absorption.

In a complementary approach focusing on direct contaminant immobilization, Mwandira et al. (2017) achieved complete bioremediation of lead (Pb^{2+}) from mine waste using Pararhodobacter sp. via MICP, which also concurrently enhanced the unconfined compressive strength of the treated sandy matrices. While chemical binders like KMP (a blend of phosphate compounds and reactive magnesia) offer an alternative stabilization method by forming insoluble metal phosphate precipitates, as shown by Xia et al. (2018), MICP presents a more biologically driven and often more sustainable pathway for simultaneous strength improvement and contaminant encapsulation.

[#]Corresponding author. E-mail address: cleomarreginatto@hotmail.com
[1]Universidade de Passo Fundo, Instituto de Tecnologia, Departamento de Geotecnia Ambiental, Passo Fundo, RS, Brasil.

Submitted on June 26, 2025; Final Acceptance on April 22, 2026; Discussion open until November 30, 2026.
Editor: Renato P. Cunha
https://doi.org/10.28927/SR.2026.010125

The function of MICP is governed by hydrolysis of urea, which is biochemical process that the bacterial ureolytic enzyme hydrolyzes the urea [$CO(NH_2)_2$)] in aqueous medium producing carbonate (CO_3^{-2}) and ammonium (NH^{4+}) ions (Follmer 2010; Kumar et al., 2023).

With the production of ammonia through ureolytic activity, the pH of the medium increases. Afterwards, it starts the process of calcite's ($CaCO_3$) formation with the interaction between carbonate ions (CO_3^{-2}) and calcium ions (Ca^{2+}), derived from the biocide solution, resulting in $CaCO_3$ (Stocks-Fischer et al., 1999; DeJong et al., 2011; Ng et al., 2012; Al Qabany et al., 2012; Shu et al., 2018; Krajewska 2018). These processes are expressed in the Equations 1 and 2.

$$CO(NH_2)_2 + 2H_2O \underset{Urease\ reaction}{\rightarrow} CO_3^{2-} + NH_4^{+} \quad (1)$$

$$Ca^{2+} + CO_3^{\ 2-} \underset{Calcite\ formation}{\rightarrow} CaCO_3(s) \quad (2)$$

Calcium ions (Ca^{2+}) have been found to promote microbial activity by decreasing the direct sorption of heavy metals in microbial cells (Fang et al., 2021; Comadran-Casas et al., 2025). In addition, the $CaCO_3$ crystals generated through MICP can encase contaminants, reducing their bioavailability and leaching into the environment (Yang et al., 2023).

The starting point of MICP was the application on sandy soils in order to increase the strength and stiffness of the material, based on the microbes, especially the bacteria *S. pasteurii* and *Bacillus pasteurii* (Stocks-Fischer et al., 1999; Whiffin et al., 2007; DeJong et al., 2011; Feng & Montoya 2015; Jiang et al., 2016; Nassar et al., 2018).

The MICP is also applied in the immobilization of toxic metals, like Zn^{2+}, As^{3+}, Pb^{2+}, Cd^{2+}, Mn^{2+}, Sr^{2+}, Ba^{2+} and Al^{3+} in soils media, by providing the encapsulation, biomineralization and promoting the upgrading of Geomechanics' properties as a Solidification/Stabilization (S/S) technique (Achal et al., 2012b; Kumari et al., 2014; Li et al., 2018; Mwandira et al., 2017; Xia et al., 2018; Comadran-Casas et al., 2025). An interesting point of the technique is use of bioaugmentation or even biostimulation of natural bacteria in the soil, in which both of them could provide improvement of strength in the soil, mainly sandy soils (Nassar et al., 2018).

For the application of this technique, some factors and variables are essential to be evaluated, such as the leaching process during the application of the biocementation solution (for example, composed mainly of urea and calcium chloride for $CaCO_3$ precipitation and the nutrient medium for biostimulation of native microorganisms), as well as the effect of toxic metals on urease and the metabolism of microorganisms present in the soil.

Based on the applications of biocementation, this research may contribute to understanding the limitations of the technique's application in metal-contaminated soils. Will the application of the technique increase the speed of contaminant movement in the soil? Will microorganisms become inactive due to the toxicity of the contaminants? And finally, will the contaminants be immobilized in the soil, in addition to increasing the strength of the sandy soil?

In this sense, this article aims to evaluate the application of the MICP technique to immobilize toxic metals (hexavalent chromium (Cr^{6+}) and cadmium (Cd^{2+}) and to improve the mechanical strength of a sandy soil.

2. Materials and methods

2.1 Soil

The soil used in the research was a sandy soil from the city of Osório, Rio Grande do Sul, Brazil, located at 29° 54' 1" S/50° 16' 26" W. This soil presents rounded grains and a uniform grain-size distribution, free of organic matter. It was classified as nonplastic uniform fine sand (SP). Mineralogical analysis showed that the sand particles were predominantly quartz. The properties of the soil are shown in Table 1.

2.2 Biocementation solution

To biostimulate the microorganisms present in soil without the necessity of bioaugmentation, the biocementation solution consisted mainly by the urea and calcium's source, according to Equation. 1 and 2. Otherwise, the constituent's nutrients were needed to biostimulate the growing of native microorganisms and to precipitate $CaCO_3$. The composing of the biocementation solution has been previously applied (Amarakoon & Kawasaki 2018; Pacheco et al., 2018, 2022) and it is presented in Table 2. The pH solution was 6.8.

Table 1. Properties of the soil.

Properties	Value
Specific gravity (-)	2.65
Uniformity coefficient (Cu)	2.11
Coefficient of curvature (Cc)	1.15
D10 (mm)	0.09
D50 (mm)	0.17
Minimum Void Ratio (e_{min})	0.60
Maximum Void Ratio (e_{max})	0.85

Table 2. Biocementation solution.

Chemical	Concentration (g/L)
Nutrient Broth	3
NH_4Cl	10
$NaHCO_3$	2.12
$(NH_2)_2CO$	30.00
$CaCl_2$	56

2.3 Metal contaminants

The concentration of toxic metals/inorganic contaminants used in the researched were based on the intervention limit proposed for an industrial area, by the Brazilian soil quality law Resolution nº 420/2009 of the Environment National Council from Brazil (Brasil, 2009). Soil contamination was determined based on the dry weight of the soil, that is, considering the mass of the soil without moisture in relation to the contaminant.

Then, the experimental concentration adopted was 2 times the limit concentration for each metal. For Cr^{6+} and Cd^{2+} the initial concentrations of 20 mg.kg^{-1} and 40 mg.kg^{-1} were used, respectively. Both contaminating solutions were prepared based on a standard commercial solution of 1000mg/L, for each metal, being ($K_2Cr_2O_7$) in deionized water and $Cd(NO_3)_2$ in HNO_3. The contaminant solutions were added to the soil (according to 2.4), contributing to a final moisture content of 10% in the test specimens.

2.4 Experimental program

The research was conducted under a full factorial 2^3 experiment, which evaluated the effect of three main factors (independent variables): Cr^{6+} (X_1), Cd^{2+} (X_2) and volume of biocementation solution (X_3), according to Table 3. All the experiments were conducted in triplicates. The volumes of solutions used, 230 ml and 460 ml, correspond to 1 and 2 times the void ratio of the specimens, respectively.

This experimental program allowed to consider the influence of toxic metals and the solution's volume on several parameters (dependent variables) as: ureolytic activity of the leached solution (e.g. pH and the leaching of Cr^{6+} and Cd^{2+} during the process of biocementation); unconfined compressive strength (UCS); scanning electron microscope-(SEM) and Energy-dispersive X-ray spectroscopy-(EDS); and alkaline/acid extraction of Cr^{6+} and Cd^{2+}.

The analyzed factors were chosen to understand their interactions with the dependent variable, mainly the factor X_3, because usually the amount required to biocement a sandy soil is related to 2x void ratio (Gomez et al., 2017; van Paassen et al., 2010). In our case, this amount could contribute to the leaching of the contaminants (X_1 and X_2). Moreover, the interaction between Cr^{6+} and Cd^{2+} was studied both in combination and separately.

By considering the experimental program, the specimens were made on columns, also called "biocementation columns" made by PVC plastic, according to Figure 1. The dimensions of the columns were: 40 cm of height and 5 cm of diameter (∅), where the internal diameter (∅) was 4.4 cm. The column had a system to collect the leached solution from the specimens and a top free layer to percolate the biocementation solution. The total layer of soil was composed by 30 cm of Osório sand, with the top layer -5 cm-, containing the contaminated soil (e.g. Cr^{6+}, Cd^{2+} or even both contaminants) and the residual layer column -25cm- with non-contaminated soil.

The biocementation solution were applied in 14 injections, within an interval of 2 days (total of 28 days), to guarantee the full development of the microorganisms and precipitation of $CaCO_3$ (Amarakoon & Kawasaki 2018; Nassar et al., 2018; van Paassen et al., 2010; Xia et al., 2018). The biocementation solution was applied via a gravity-fed percolation method.

The soil used was initially unsaturated and natural percolation was applied. For each injection, the designated volume of solution (corresponding to 1x or 2x the void ratio) was poured directly onto the top surface of the soil column.

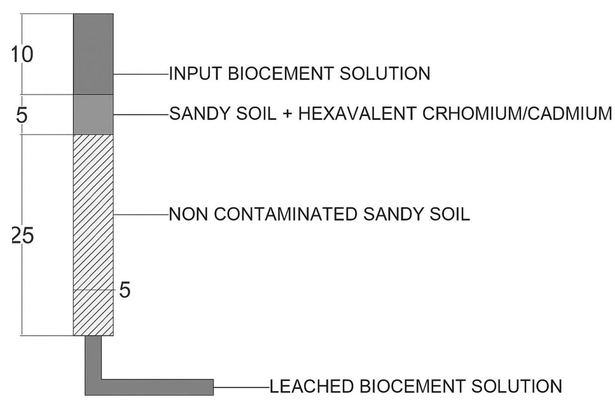

Figure 1. Biocementation design.

Table 3. Experimental full factorial 2^3 program matrix.

Run	Experiment Coded Runs	Coded Factors			Non-Coded Factors		
		X_1 [Cr^{6+}]	X_2 [Cd^{2+}]	X_3 [Volume of Solution]	X_1 [Cr^{6+}] (mg.kg^{-1})	X_2 [Cd^{2+}] (mg.kg^{-1})	X_3 [Volume of Solution] (mL)
1	A01 (Control)	-1	-1	-1	0	0	1x void ratio
2	A02	+1	-1	-1	20	0	1x void ratio
3	A03	-1	+1	-1	0	40	1x void ratio
4	A04	+1	+1	-1	20	40	1x void ratio
5	B01 (Control)	-1	-1	+1	0	0	2x void ratio
6	B02	+1	-1	+1	20	0	2x void ratio
7	B03	-1	+1	+1	0	40	2x void ratio
8	B04	+1	+1	+1	20	40	2x void ratio

The solution was allowed to drain freely under gravity, and the leachate was collected from the bottom outlet for analysis. Furthermore, the injections for each specimen were performed sequentially at two-day intervals. This injection procedure was repeated 14 times for each column, resulting in a total treatment period of 28 days. This protocol, adapted from Amarakoon & Kawasaki (2018) and van Paassen et al. (2010), was designed to prevent ammonia inhibition and near-injection-point clogging, thereby promoting uniform microbial activity and calcite precipitation throughout the column.

The experimentation was conducted under room temperature of 23 °C (average temperature for the natural soil). Another two parameters for the molding process, the relative density (%) and the initial moisture content (%) were respectively: 50% and 10%.

2.5 Monitoring of ureolytic activity

Following each injection and subsequent percolation of the biocementation solution, the pH of the leachate collected from the columns was measured using a bench-top pH meter. Leachate samples were collected in 500 mL beakers.

The leaching of Cr^{6+} and Cd^{2+} during the process of biocementation was analyzed by the collected samples from the 14 injections of biocementation solution throughout the specimens. The amount of Cr^{6+} leached was determined by the method 7196a (USEPA, 1992). The amount of Cd^{2+} leached was determined in agreement with ASTM D4691 (ASTM, 2017).

2.6 Unconfined compressive strength (UCS)

After the process of biocementation a curing process of 28 days was adopted, in a room temperature of 23 °C (Ng et al., 2012; Al Qabany et al., 2012). This time was defined as representing the usual curing period for cementitious materials, for resistance to gain. Because of the dimensions of the specimens (e.g. columns 30 cm of height and 4.4 cm of diameter), and according to ASTM D2166/D2166M-13 (ASTM, 2013) for unconfined and undrained compression test, to obtain a minimum length-to-diameter ratio of 2:1, the specimens were sectioned in three segments' horizons: "Top" (0-10 cm of length; initially contaminated soil + initially non contaminated soil); "Medium" (10-20 cm of length; initially non contaminated soil); and "Bottom" (20-30 cm of length; initially non contaminated).

2.7 Alkaline and acid digestion

The alkaline and acid digestion were conducted on the "Top", "Medium" and "Bottom" layers. It means that samples were taken from 3 different depths to extract the contaminants all along the specimens. These extractions were made punctually at 5, 15 and 25 cm as the top, medium and bottom layers, respectively. In order to extract Cr^{6+} from the bioremediated specimens (e.g. accordingly to Table 3), the alkaline digestion was used based on the method 3060a was used (USEPA, 1996b) in complement with the method 7196a (USEPA, 1992). The extraction of Cd^{2+} from the specimens (e.g. accordingly to Table 3) was based on method 3050B (USEPA, 1996a) in complement with ASTM D4691 (ASTM, 2017) (Grigalavičiene et al., 2005; Hu et al., 2006).

2.8 SEM EDS analysis

The microstructure formed between the sandy soil, $CaCO_3$, Cr^{6+} and Cd^{2+} was analyzed by scanning electron microscope (SEM) equipped with Energy-dispersive X-ray spectroscopy (EDS). Mainly, this procedure consisted of identifying the biomineralization of $CaCO_3$, $Cr(CO_3)_3$ and $CdCO_3$ (Achal et al., 2012a; Zhu et al., 2016; Xia et al., 2018). For that, samples were collected from the top layer of the specimens, due to the soil being initially contaminated. The analyses were conducted under high vacuum conditions at an accelerating voltage of 15 kV and a working distance of approximately 10 mm, and the samples were oven-dried in a forced-air oven at 60 °C for 24 hours to remove moisture. Under these conditions, the instrument's resolution is 3.0 nm. This procedure aimed to identify the biomineralization of $CaCO_3$ and the potential precipitation of Cr- and Cd-carbonates (Achal et al., 2012a; Zhu et al., 2016; Xia et al., 2018).

2.9 Statistical analysis

All experiments were performed in triplicate. The data were statistically analyzed using analysis of variance (ANOVA), and the means were compared by Tukey's test with the Statistica 8 software (StatSoft®, USA).

3. Results and discussion

3.1 Monitoring of ureolytic activity

The process of biocementation is affected by many factors [e.g. pH, nutrients, molarity of solution, temperature among others]. The hydrolysis of urea, typically catalyzed by the enzyme urease, directly releases ammonia (NH_3) and carbon dioxide (CO_2), which in aqueous solution form ammonium ions (NH_4^+), bicarbonate ions (HCO_3^-), and hydroxide ions (OH^-), leading to a predictable increase in the pH and alkalinity of the medium (Al Qabany et al., 2012; Anbu et al., 2016; Gomez et al., 2017). That's why the monitoring process is necessary to evaluate the activity of the bacteria or native microorganism in the soil (Yasuhara et al., 2012; Phillips et al., 2013). The mean of pH of the leached solution during the application of the biocement solution is shown in the Figure 2.

The ureolytic activity of the biostimulated bacteria on soil varied accordingly to the pH, in its change from neutral stages [(e.g. by considering the initial pH of solution at 6.8 (Table 2)] to alkaline stages (from around 7 to around 8 - Figure 2). All the tested specimens had an alkaline stage, indicating by that the occurrence of biocementation. It's important to notice that the Cr^{6+} and Cd^{2+} could be toxic for the bacteria in the soil. In this case, these toxic metals did not affect directly in the development phase and process of urease of the bacteria (Kang & So 2016; Mwandira et al., 2017).

By the results of pH and its variance along the treatment, according to Kang & So (2016), Mwandira et. al (2017), Cheng et al. (2014) and Jiang et al. (2016) the ureolytic activity could be associated with the progress of pH from neutral to alkaline. This process indicates, by analyzing Figure 2, that ureolytic activity of the biostimulated bacteria had increased specially from injection 4.

The statistical analysis showed that the influence of Cr^{6+}(X1), Cd^{2+}(X2) and volume of solution (X3) were significative p-value were 10^{-4}, 0.03, 0.01, respectively on the pH`s effect, according to Table 4.

By that, it's possible to observe that the specimens with 1x void ratio's volume solution had alkaline increased around the injection 5 (at day 10) and the specimens with 2x void ratios had the alkaline increased at the injection 12. That means that nutrient availability in specimens with 2x void ratio enables urease production for longer time, precisely due to nutrient availability higher than 1x void ratio and it infers on the mitigation of heterogeneity caused by the technique. Furthermore, the presence of Cr^{6+} and Cd^{2+} influence on the pH of the leached, but it did not mitigate the process of biocementation by allowing the alkaline stages accordingly to the increase of the pH during the stimulation or also called the process of biocementation (He et al., 2019; Rajasekar et al., 2021) .The monitoring process analyzed the leaching of the Cr^{6+} and Cd^{2+} during the process of biocementation, according to Figures 3 and 4.

The biocementation solution and the technique could promote the leaching process of the contaminants present in the soil, especially because of the sandy soil, in this case within high permeability. So, the leaching process of Cr^{6+} was higher in comparison of Cd^{2+}, especially on specimen A02, within less volume of solution and no presence of Cd^{2+}.

This could be associated to a reaction of Cr^{6+} and Cd^{2+}, which leaded to retention of the contaminant or also associated to the degree of biocementation on the top layer of these specifics specimens, or also the immobilization by the biomineralization which could create another minerals as $Cr(CO_3)_3$ and $CdCO_3$ (Kumari et al., 2014; Kang et al., 2014; Khadim et al., 2019; Omoregie et al., 2024). The specimen A02 (e.g. which the residual concentration of Cr^{6+} was 62.67%), the other specimens (e.g. A04, B02 and B04) retained, respectively 85.53, 85.45 and 87.05%, of the residual concentration of Cr^{6+} on the column, which means not leached in the biocementation solution during the process of application

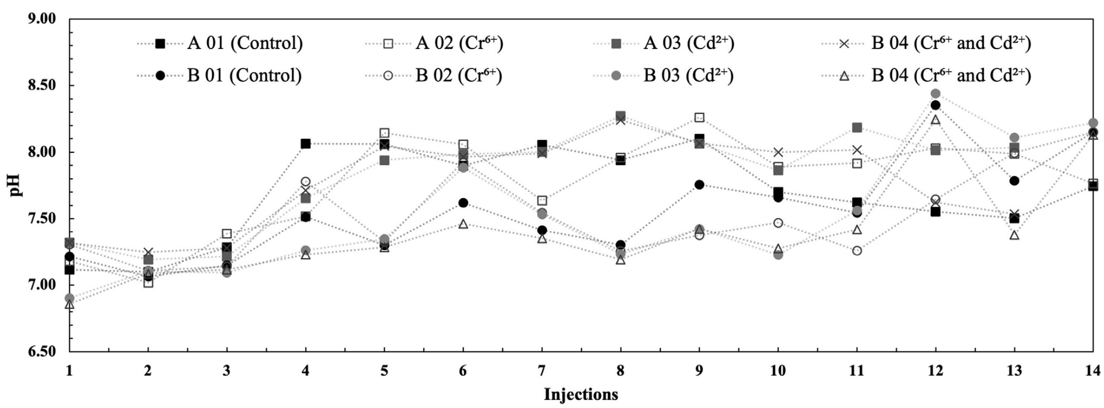

Figure 2. Monitoring of pH from the biocement leached solution.

Table 4. pH ANOVA matrix.

Effect	Test	F	DF	p-value
Intercept	Wilks	4097224	13	0.000387
Cr^{6+}(X1)	Wilks	518	13	0.034362
Cd^{2+}(X2)	Wilks	1697	13	0.018996
Volume of Solution (X3)	Wilks	10824	13	0.007523
(X1) vs (X2)	Wilks	21	13	0.169919
(X1) vs (X3)	Wilks	15	13	0.198118
(X2) vs (X3)	Wilks	1435	13	0.020660
(X1) vs (X2) vs (X3)	Wilks	386	13	0.039816

The statistical analysis indicated the significant influence of Cr^{6+}(X_1), Cd^{2+} (X_2) and volume of solution (X_3) (e.g. p value under 0.05 for all cases) on the leaching process, which infers to conclude that the Cr^{6+} and Cd^{2+} had and specific interaction on the leaching process, being more effective the MICP's technique when applied for the both metals simultaneously.

The analysis of Figure 4 shows a specific scenario where the leaching is more accentuated for specimens B03 and B04, the ones with 2x void ratio, indicating that the X_3 has a significatively influence on the leaching process, what is supported by the statistical analysis where the X_3 is significant within a p value < 10^{-8} and also is X_2 with a p value bellow 0.05. Meantime, it is important to highlight that the residual concentration of Cd^{2+} for all the specimens were higher than 92% and those which presented higher leaching (e.g. B03 and B04) received more nutrients and chemical compounds by the solution which leads to more homogeneous biocementation all along the columns.

The integration of heavy metal ions into the evolving $CaCO_3$ structure is pivotal to the effectiveness of MICP. The Cd^{2+} and Cr^{6+} stabilization is linked to the formation of metal carbonates ($Cr(CO_3)_3$ and CdC_{O3}). This process involves mechanisms such as isomorphic substitution of Ca^{2+}or incorporation into crystal lattice interstices or defects (Tamayo-Figueroa et al., 2019). This incorporation depends on the ionic radius and charge of the heavy metal ions, which influence their ability to substitute for Ca^{2+}in the lattice. The High saturation of $CaCO_3$ in the environment promotes nucleation and growth of $CaCO_3$ crystals, enhancing the entrapment of heavy metals, conversely, low saturation levels may inhibit these processes, reducing immobilization efficiency (Omoregie et al., 2024).

The substitution of Ca^{2+} by comparable ionic radii such as Pb^{2+}, Cd^{2+}, or Zn^{2+} tends to be more efficient compared with metals with significantly different ionic radii or charges (e.g., Cr^{3+}, Cr^{6+}) (Mitra et al., 2022). This relationship justifies the greater leaching of hexavalent chromium in relation to cadmium in the experiments.

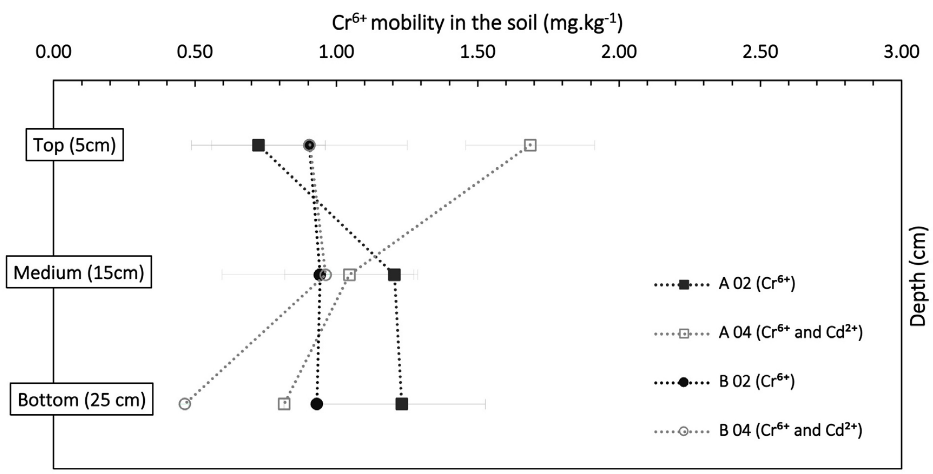

Figure 3. Residual concentration of Cr^{6+} in the specimens at different depths for 1x and 2x void ratios.

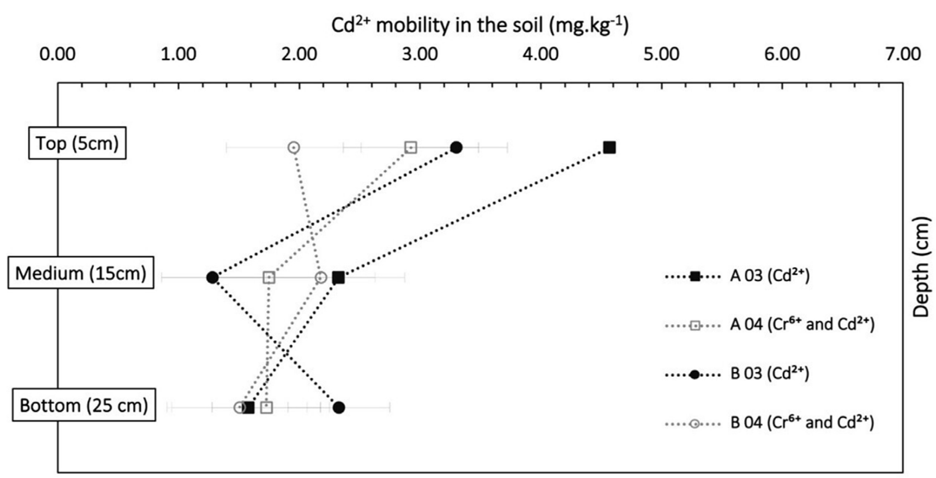

Figure 4. Residual concentration of Cd^{2+} in the specimens at different depths for 1x and 2x void ratios.

3.2 Unconfined compressive strength (UCS)

The unconfined compressive strength is summarized in Figure 5.

The experimental results ranged from 114.84 to 917.43 kPa (e.g. being respectively 0.11 and 0.92 MPa), providing for the samples improvement of geomechanical strength and also according to previous experiments, which varied from 0.2 to 20 MPa in sandy soil without contaminants (van Paassen et al., 2010; Al Qabany et al., 2012) and from 1.33 to 2.87 MPa for contaminated soils (Mwandira et al., 2017). Also, the result could be compared to the Osório sand cemented with 3% of Portland cement by reaching the magnitudes between 0.60 to 0.75 MPa (Forcelini et al., 2016).

In this work, it's important to notice that the columns allowed sampling from three 3 different depths ("Top", "Medium" and "Bottom"). Also, the statistical analysis was calculated for the "top" layer, due to the availability of specimen molding for all the runs.

Statistically the volume of solution (X_3) was not significant for the "top" layer which means that for superficial depths the MICP's technique does not require more than 1x void ratio for the improvement of geomechanical strength, even when contaminants were present (e.g., A02, A03, A04, B02, B03, B04). Otherwise, the presence of Cr^{6+}(X_1) and Cd^{2+}(X_2) were significative (e.g. p value< 10^{-3} and <10^{-5} respectively) for the UCS' results, accordingly to Table 5.

This corroborates and opens prerogatives to the claim that metallic contaminants influence the structure of $CaCO_3$ formed through biocementation, through the effect of biominerization and composition of new minerals such as $Cr(CO_3)_3$ and $CdCO_3$ affecting the biomineralization process. But even being significative, for the strength properties of the soil, by analyzing together with the results obtained in the monitoring process (e.g., 3.1), it can be inferred that the biocement was effective not only in the immobilization of the metals in the cementation columns, but also as a means of geomechanical soil improvement, even in the presence of Cr^{6+} and Cd^{2+} (He et al., 2019; Gebru et al., 2021; Lai et al., 2021; Rajasekar et al., 2021).

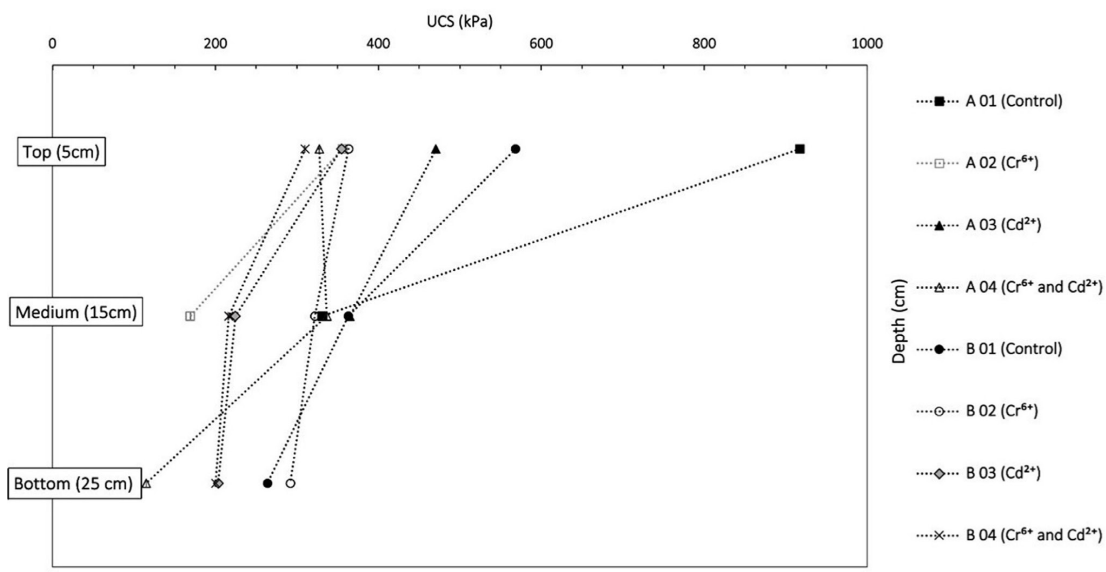

Figure 5. Unconfined compression strength in the specimens at different depths for 1x and 2x void ratios.

Table 5. UCS ANOVA matrix.

Effect	SS	MS	F	p-value
Intercept	4296260	4296260	632.0207	<0.05
Cr^{6+}(X_1)	116976	116976	17.2083	0.001985
Cd^{2+}(X_2)	296738	296738	43.6529	0.000060
Volume of Solution (X_3)	8284	8284	1.2186	0.295492
(X_1) vs (X_2)	21337	21337	3.1389	0.106860
(X_1) vs (X_3)	155106	155106	22.8176	0.000749
(X_2) vs (X_3)	84441	2314	0.3404	0.572520
(X_1) vs (X_2) vs (X_3)	67977	84441	12.4221	0.005497
Error	67977	6798		

The volume of the solution was not statistically significant for the "top" layer, but when applied 2x void ratio of biocementation solution the biocementation was improved and occurred more homogeneously, ensuring sampling all long the biocement columns because of the improvement on the strength until the "bottom" layer; otherwise, the specimens with 1x void ratio just allowed sampling until the "medium" layer because of the poor biocementation associated with the depth.

In the specimens with 2x void ratio, the presence of contaminants did not interfere in the process of biocementation along the specimens, ensuring resistance to them throughout the column and providing higher UCS' value at "bottom" layer, for the case of B02 with 292.09 kPa in comparison with 263.87 KPa for B01 (e.g., non-contaminated). So, to complement these findings, it is important to analyze the effective presence of Cr^{6+} and Cd^{2+} within the $CaCO_3$ structure, what is discussed on the following topics.

3.3 Contamination mobility in the soil

The punctual analyses of the different specimens are shown in Figures 6 and 7.

These analyses were conducted to identify the mobility of Cr^{6+} and Cd^{2+} throughout the columns and to reassure the presence of the contaminants at different depths and their biomineralization and ion interaction with the calcium carbonate.

The Figures 6 and 7, show that Cr^{6+} was able to be transported through the column from top layer (originally contaminated) to non-contaminated soil originally, the bottom layer. The specimen A04 (contaminated by Cr^{6+} and Cd^{2+}) presented the highest amount of Cr^{6+} at the top layer, being 1.69 $mg.kg^{-1}$ (e.g. 8.45% of the initial concentration) which corroborates to the discussion that there is an interaction between Cr^{6+} and Cd^{2+} that improves the immobilization of Cr^{6+}. Also, the volume of solution (X_3) did not interfere directly in the transport of Cr^{6+}.

These results also contribute to the discussion that occurred the biomineralization of $Cr(CO_3)_3$ in all depths but also associated with the increase of strength by UCS's test and the capability of native microorganisms to precipitated $CaCO_3$ in the absence and in the presence of Cr^{6+}.

The same analogy was conducted to the soil contaminated with cadmium where is possible to identify that Cd^{2+} was transported through the column of biocementation. The most immobilized contaminant was A03 in absence of Cr^{6+} by containing 4.57 $mg.kg^{-1}$ (e.g. 11.42% of the initial concentration) which indicates that for the Cd^{2+}, the presence or absence of Cr^{6+} did not interfere in the transport of the contaminant. Otherwise, the mobility of Cd^{2+} demonstrated to be less active, which is correlated in the leached amount of the contaminant.

The Cd^{2+} were found along the depths of the columns, and the biomineralization of $CdCO_3$ by the production of CaCO3 was efficient even in the presence of the contaminant, proving the capability of the native microorganism (Khadim et al., 2019). The concentration was not toxic for the metabolism of microorganisms as well. Still, there was not significative difference in the transport in comparison with the volume of solution (X3) (Kumari et al., 2014; He et al., 2019).

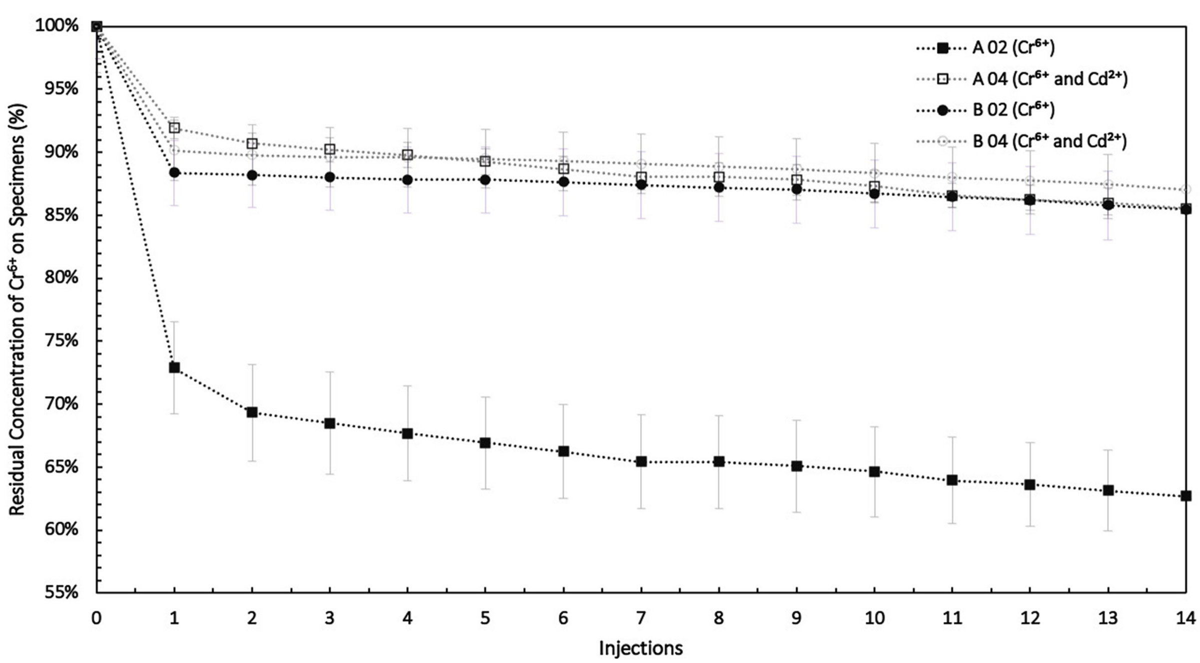

Figure 6. Residual value of contaminant along the soil column (chromium isolated and with cadmium) in the specimens for 1x and 2x void ratios.

These results ensure the geomechanical strength of the contaminated soil, the capability of Cr^{6+} and Cd^{2+} immobilization and the formation of $Cr(CO_3)_3$ and $CdCO_3$ within proper geomechanical strength and stiffness of the structure of these biominerals.

Then, Figure 8 presents the rate of immobilization of the Cr^{6+} and Cd^{2+} promoted by the biostimulation of native microorganisms.

It allows to observe the lowest result of immobilization of approximately 2/3 for the sample A02 and the highest

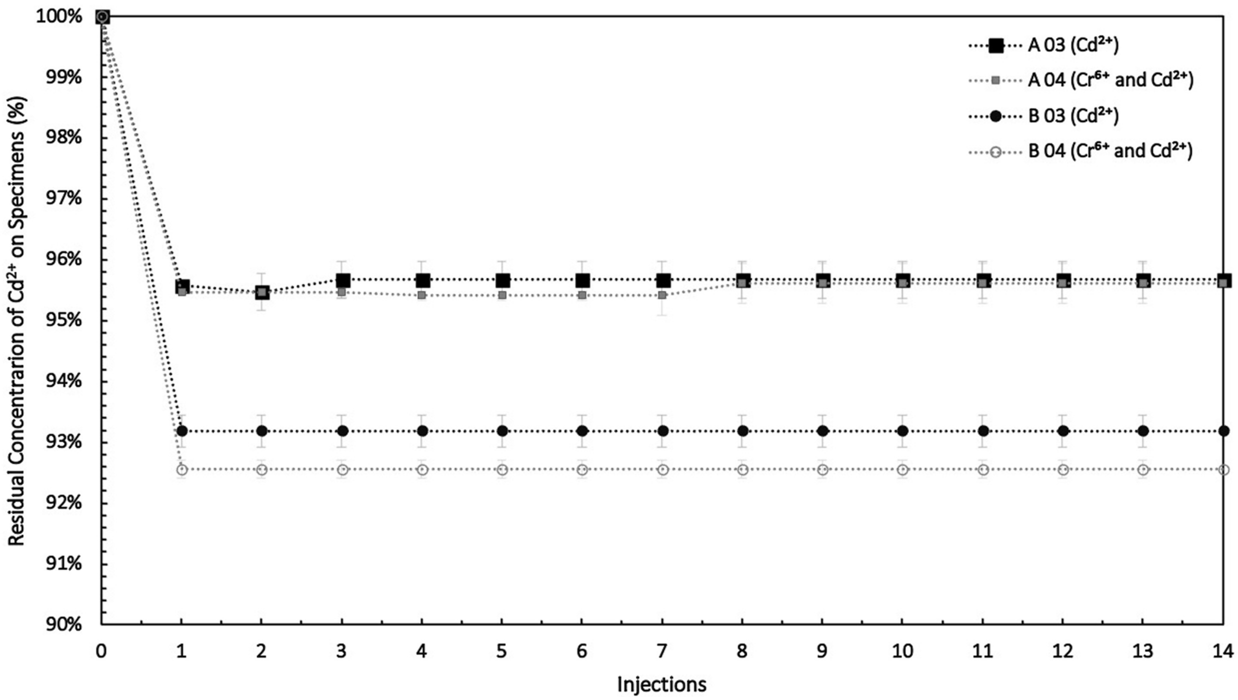

Figure 7. Residual value of contaminant along the soil column (cadmium isolated and with chromium) in the specimens for 1x and 2x void ratios.

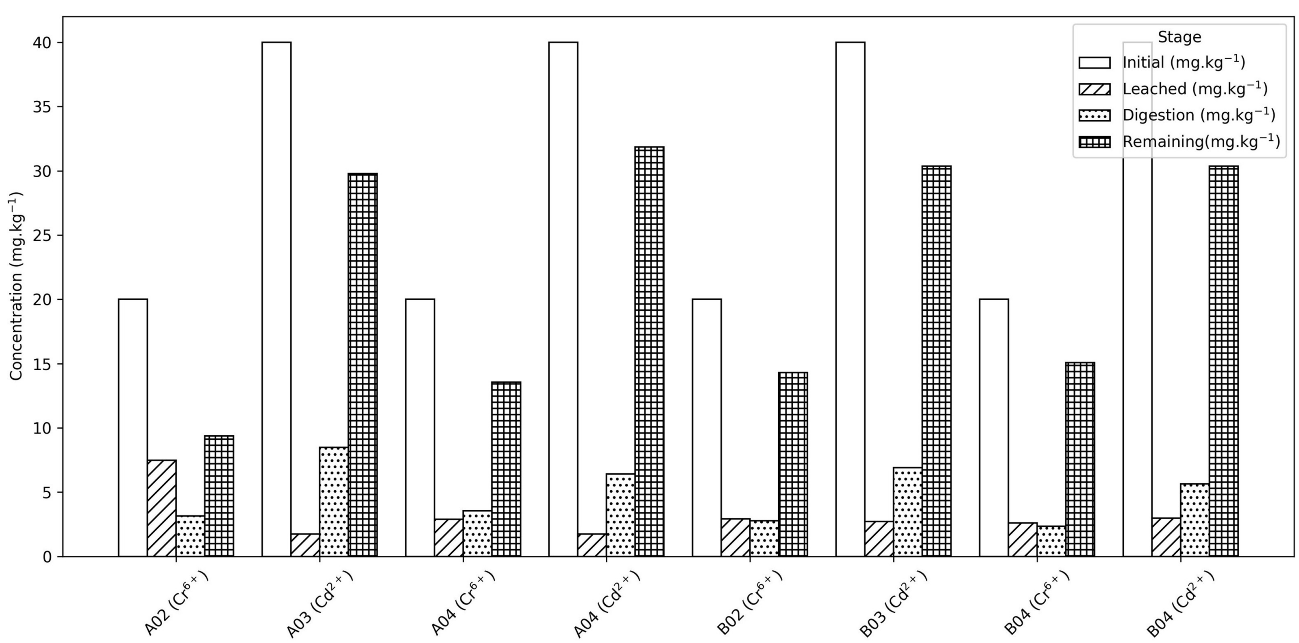

Figure 8. Mass balance off the contaminants in the soil in the specimens for 1x and 2x void ratios.

concentration remaining in the sample A03, about 90% of the initial concentration. This also considered the punctual extraction (e.g. demonstrative) of contaminants from specimens. By that is assured the capability of biomineralization of the studied contaminants and the best efficiency on this parameter is also found by Cd^{2+} contamination. This occurs because during the process of MICP, heavy metals with divalent ions such as Cd^{2+} are substituted for Ca^{2+} which results in the precipitation of heavy metal carbonates thus converting them from a bioavailable to a non-bioavailable.

Other studies demonstrates that metals such as lead (Pb^{2+}), cobalt (Co^{2+}) chromium (Cr^{2+}), cadmium (Cd^{2+}) and copper (Cu^{2+}) share similar divalent ion formation as calcium (Ca^{2+}) and have a large surface area and the abundance of negative ions on the cell surface (Kang et al., 2014; Maity et al., 2019; Rajasekar et al., 2021).

3.4 SEM-EDS analysis

To analyze specimen patterns, SEM-EDS analysis, shown in Figure 9, where part (A) and (B) show specimen A01 (control) in the absence of contaminants; (C) and (D) show the results for sample A02 contaminated with Cr^{6+}; and, (E), and (F), show the results for sample A03, contaminated with Cd^{2+}.

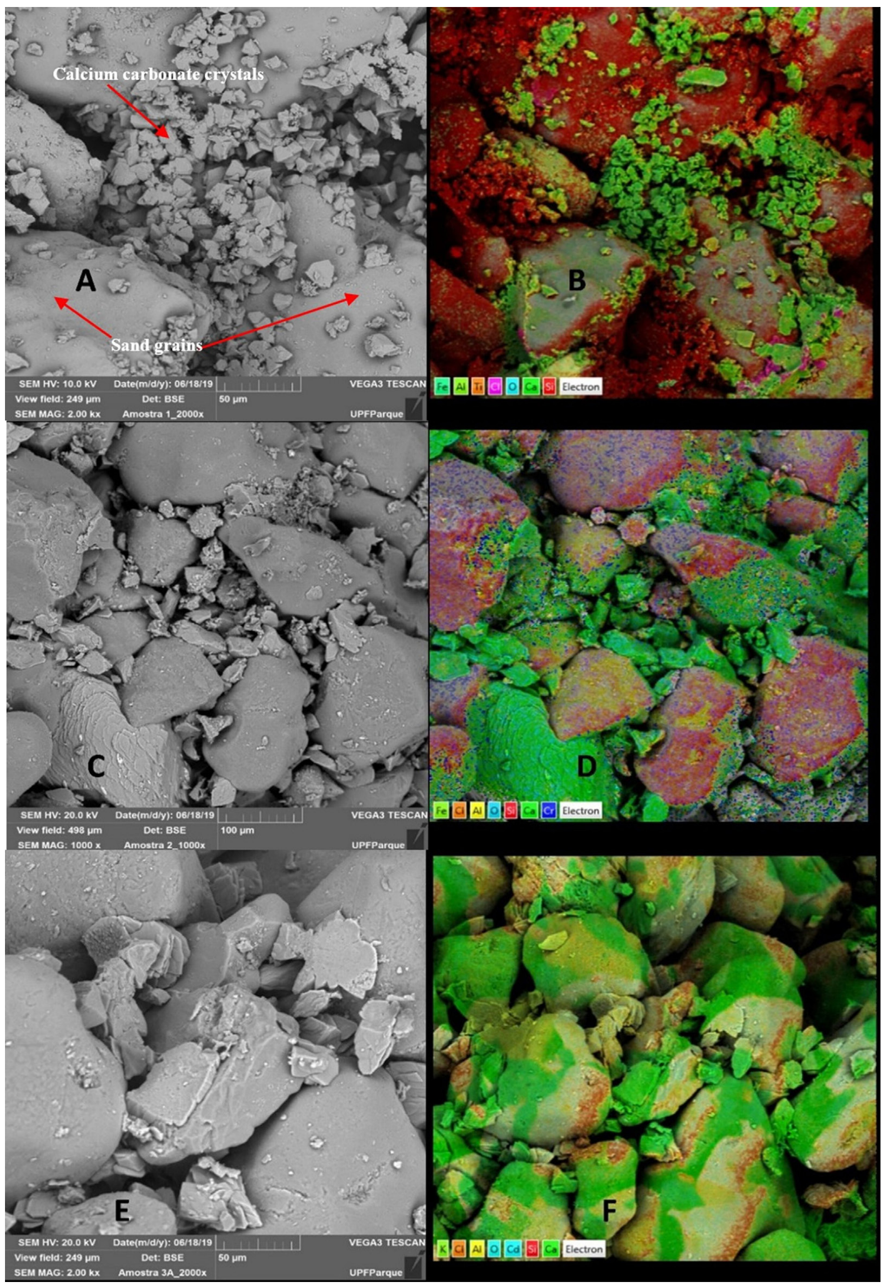

Figure 9. Scanning electron microscope of control and, SEM-EDS layered image with the elements of specimen with and without contaminants.

In the Figure 9A is possible to identify the product of biocementation as a bond to the grains of the soil. This conception brings to the soil the increase of geomechanical strength via the crystallization of $CaCO_3$ alongside the grains (Achal et al., 2013; Zhu et al., 2016; Mwandira et al., 2017).

The crystals were roughly rhombohedral in their shapes; and to confirm the biocementation by biostimulation of natural microorganisms, analysis of SEM and EDS were combined, to indicate the accumulation of minerals. Then, by Figure 9B it is possible to identify Ca and O, and elements of the original soil, by containing high amounts of the essential elements for the precipitation of $CaCO_3$.

In the Figures 9C and 9D it is possible to identify the natural grains of soil surrounded by $CaCO_3$; providing then the result of biocementation by rhombohedral shapes. But it is also possible to notice the presence of the Cr^{6+} on the surface of $CaCO_3$, which means that possibly was an interaction between $CaCO_3$ and Cr^{6+} by generating the element $Cr(CO_3)_3$ by the isomorphic substitution of Ca to Cr^{6+}. The probability of this kind of interaction is passive to happen in the MICP environment along with contaminants as Cr^{6+} and Cd^{2+} and specially by the presence of ureolytic bacterias (He et al., 2019; Khadim et al., 2019; Kumari et al., 2014).

Thus, in addition to improving geomechanical strength characteristics, the use of MICP can immobilize contaminants, as a solidification and stabilization technique.

Furthermore, the result from Figure 9D identified the amount of Ca (dark green color) and O (Light blue color), which indicates the presence of $CaCO_3$, but also showed amounts of $Cr^{6+,}$ which leads to conclude that even with the leaching process (topic 3.1) during the application of the biocementation solution, there is still contaminant on the top layer and formed $Cr(CO_3)_3$ by the biostimulation of native microorganisms.

Still, Figures 9E and 9f has identified the precipitated forms of CaCO3 produced by the native microorganisms in the specimen A03 (Cd^{2+} contaminated). This precipitation consisted in chemical bonds between the soil's grains within rhombohedral shapes as well. It is also possible to notice, especially by Figures 9E and 9f the presence of Cd^{2+} on the surface of the grain (e.g. noted in small amount and mixed within the different tones of green), within the $CaCO_3$, which leads to conclude and observe availability to form $CdCO_3$ by MICP's process, by the isomorphic substitution of Ca to Cd^{2+} (Kang et al., 2014; Khadim et al., 2019; Kumari et al., 2014).

Also, the patterns from Figure 9F indicates the formation of $CaCO_3$ by the large amount of Ca and O founded on the sample and it also infers the presence of Cd^{2+} on the specimen, indicating that the contaminant was still encapsulated on the top layer, even though it could be transported to the under layers (topic 3.4).

Furthermore, the co-precipitaion of Cd^{2+} in during the formation of $CaCO_3$ was studied by Lyu et al. (2022), and it demonstrated the capability and bioavailability in remediated soils to eliminate the interference within Ca^{2+}. This process could be associated with co-precipitation resulted in this present research, in which the leaching process was farther controlled due the co-precipitation of Cd^{2+} and increasing the pH of the leached biocementation solution. (Landa-Marbán et al., 2021).

4. Conclusions

Based on the experimental results, the following conclusions can be drawn:

* The native soil microorganisms were successfully biostimulated to induce the precipitation of $CaCO_3$, while simultaneously contributing to the immobilization of Cr^{6+} and Cd^{2+}. SEM-EDS analysis confirmed the precipitation of calcite and its association with the metal contaminants, suggesting the primary mechanisms of immobilization were encapsulation within the calcite matrix and coprecipitation via isomorphic substitution (for Cd^{2+});
* The native soil microorganisms produced the precipitation of $CaCO_3$ by biostimulation while immobilizing Cr^{6+} and Cd^{2+};
* The immobilization of Cr^{6+} and Cd^{2+} likely occurred through their incorporation into carbonate minerals, supported by the chemical conditions created by the biocementation process;
* There is leaching of contaminants from the contaminated soil to the uncontaminated soil during the application of MICP. This occurs in the first injections while biocement has not yet formed. The values are higher for hexavalent chromium than for cadmium.
* Even in the presence of contaminants, there was precipitation of calcium carbonate and consequent improvement in mechanical strength. The volume of biocementation solution was not statistically significant for the upper layer. However, doubling the volume of this variable provided an improvement in the homogeneity of the technique, ensuring more homogeneous precipitation of calcium carbonate throughout the 30 cm of the biocementation column.
* The MICP technique proved effective in contaminated sandy soil, promoting biocementation and metal retention. Furthermore, there was an increase in soil strength. Thus, the technique could be a sustainable application option for contaminated soil, with the help of natural soil microorganisms.

Declaration of interest

The authors have no conflicts of interest to declare. All co-authors have observed and affirmed the contents of the paper and there is no financial interest to report.

Authors' contributions

Vinicius Luiz Pacheco: conceptualization, data curation, investigation, methodology, formal analysis, validation, writing – original draft. Cleomar Reginatto: conceptualization, supervision investigation, methodology, formal analysis, writing – review and editing. Antônio Thomé: conceptualization, project administration, funding acquisition, writing – review and editing.

Data availability

All data produced or examined in the course of the current study are included in this article.

Declaration of use of generative artificial intelligence

This work was prepared without the assistance of any generative artificial intelligence (GenAI) tools or services. All aspects of the manuscript were developed solely by the authors, who take full responsibility for the content of this publication.

List of symbols and abbreviations

ANOVA	Analysis of variance
ASTM	American Society for Testing and Materials
Ca^{2+}	Calcium ion
$CaCl_2$	Calcium chloride
$CaCO_3$	Calcium carbonate
Cd^{2+}	Divalent cadmium ion
$CdCO_3$	Cadmium carbonate
$Cd(NO_3)_2$	Cadmium nitrate
CO_3^{2-}	Carbonate ion
$CO(NH_2)_2)$	Urea
CONAMA	Environment National Council from Brazil
$Cr(CO_3)_3$	Chromium (III) carbonate
Cr^{6+}	Hexavalent chromium
H_2O	Water
HNO_3	Nitric acid
$K_2Cr_2O_7$	Potassium dichromate
Kpa	Kilopascal
MICP	Microbially induced calcite precipitation
MPA	Megapascal
$NaHCO_3$	Baking soda
NH_4^+	Ammonium ion
NH_4Cl	Ammonium chloride
SEM/EDS	Scanning Electron Microscopy/Energy Dispersive Spectroscopy
UCS	Unconfined Compressive Strength
USA	United States of America

References

Achal, V., Mukherjee, A., Basu, P.C., & Reddy, M.S. (2009). Strain improvement of *Sporosarcina pasteurii* for enhanced urease and calcite production. *Journal of Industrial Microbiology & Biotechnology*, 36(7), 981-988. https://doi.org/10.1007/s10295-009-0578-z.

Achal, V., Pan, X., Fu, Q., & Zhang, D. (2012a). Biomineralization based remediation of As(III) contaminated soil by *Sporosarcina ginsengisoli*. *Journal of Hazardous Materials*, 201-202, 178-184. https://doi.org/10.1016/j.jhazmat.2011.11.067.

Achal, V., Pan, X., Zhang, D., & Fu, Q. (2012b). Bioremediation of Pb-contaminated soil based on microbially induced calcite precipitation. *Journal of Microbiology and Biotechnology*, 22(2), 244-247. https://doi.org/10.4014/jmb.1108.08033.

Achal, V., Pan, X., Lee, D.J., Kumari, D., & Zhang, D. (2013). Remediation of Cr(VI) from chromium slag by biocementation. *Chemosphere*, 93(7), 1352-1358. https://doi.org/10.1016/j.chemosphere.2013.08.008.

Al Qabany, A., Soga, K., & Santamarina, C. (2012). Factors affecting efficiency of microbially induced calcite precipitation. *Journal of Geotechnical and Geoenvironmental Engineering*, 138(8), 992-1001. https://doi.org/10.1061/(ASCE)GT.1943-5606.0000666.

Al-Salloum, Y., Hadi, S., Abbas, H., Almusallam, T., & Moslem, M.A. (2017). Bio-induction and bioremediation of cementitious composites using microbial mineral precipitation: a review. *Construction & Building Materials*, 154, 857-876. https://doi.org/10.1016/j.conbuildmat.2017.07.203.

Amarakoon, G.G.N.N., & Kawasaki, S. (2018). Factors Affecting Sand Solidiflcation Using MICP with Pararhodobacter sp. *Materials Transactions*, 59(1), 72-81. https://doi.org/10.2320/matertrans.M-M2017849.

Anbu, P., Kang, C.H., Shin, Y.J., & So, J.S. (2016). Formations of calcium carbonate minerals by bacteria and its multiple applications. *SpringerPlus*, 5(1), 250. https://doi.org/10.1186/s40064-016-1869-2.

ASTM D2166/D2166M-13. (2013). *Standard test method for unconfined compressive strength of cohesive soil*. ASTM International, West Conshohocken, PA. https://doi.org/10.1520/D2166-06

ASTM D4691. (2017). *Standard practice for measuring elements in water by flame atomic absorption spectrophotometry.* ASTM International, West Conshohocken, PA. https://doi.org/10.1520/D4691-17.

Brasil. Conselho Nacional do Meio Ambiente – CONAMA. (December 30, 2009). Resolução CONAMA nº 420 de 28/12/2009. Dispõe sobre critérios e valores orientadores de qualidade do solo quanto à presença de substâncias químicas e estabelece diretrizes para o gerenciamento ambiental de áreas contaminadas por essas substâncias em decorrência de atividades antrópicas. *Diário Oficial [da] República Federativa do Brasil*.

Chen, M., Cao, D., Li, B., Pang, H., & Zheng, C. (2023). Sodium citrate increases the aggregation capacity of calcium ions during microbial mineralization to accelerate the formation of calcium carbonate. *Environmental Research*, 224, 115479. https://doi.org/10.1016/j.envres.2023.115479.

Cheng, L., Shahin, M.A., & Cord-Ruwisch, R. (2014). Soil Stabilisation by Microbial-Induced Calcite Precipitation (MICP): investigation into some physical and environmental aspects. In *Proceedings of the 7th International Congress on Environmental Geotechnics* (pp. 1105-1112), Melbourne, Australia. ISSMGE.

Comadran-Casas, C.C., Unluer, C., Bass, A.M., MacDonald, J., Najafi, E.K., Spruzeniece, L., & Gauchotte-Lindsay, C. (2025). Bioremediation of multiple heavy metals through biostimulation of microbial-induced calcite precipitation at varying calcium-to-urea concentrations. *Journal of Hazardous Materials*, 491, 137691. https://doi.org/10.1016/j.jhazmat.2025.137691.

DeJong, J.T., Soga, K., Banwart, S.A., Whalley, W.R., Ginn, T.R., Nelson, D.C., Mortensen, B.M., Martinez, B.C., & Barkouki, T. (2011). Soil engineering in vivo: harnessing natural biogeochemical systems for sustainable, multi-functional engineering solutions. *Journal of the Royal Society, Interface*, 8(54), 1-15. https://doi.org/10.1098/rsif.2010.0270.

Fang, L., Niu, Q., Cheng, L., Jiang, J., Yu, Y.Y., Chu, J., Achal, V., & You, T. (2021). Ca-mediated alleviation of Cd^{2+} induced toxicity and improved Cd^{2+} biomineralization by Sporosarcina pasteurii. *The Science of the Total Environment*, 787(15), 147627. https://doi.org/10.1016/j.scitotenv.2021.147627.

Feng, K., & Montoya, B.M. (2015). Drained shear strength of MICP sand at varying cementation levels. In *Proceedings of the International Foundations Congress and Equipment Expo* (pp. 2242-2251), San Antonio, Texas. ASCE. https://doi.org/10.1061/9780784479087.208.

Follmer, C. (2010). Ureases as a target for the treatment of gastric and urinary infections. *Journal of Clinical Pathology*, 63(5), 424-430. https://doi.org/10.1136/jcp.2009.072595.

Forcelini, M., Garbin, G.R., Faro, V.P., & Consoli, N. C. (2016). Mechanical behavior of soil cement blends with osorio sand. *Procedia Engineering*, 143, 75-81. https://doi.org/10.1016/j.proeng.2016.06.010.

Gebru, K.A., Kidanemariam, T.G., & Gebretinsae, H.K. (2021). Bio-cement production using microbially induced calcite precipitation (MICP) method: a review. *Chemical Engineering Science*, 238, 116610. https://doi.org/10.1016/j.ces.2021.116610.

Gomez, M.G., Anderson, C.M., Graddy, C.M.R., DeJong, J.T., Nelson, D.C., & Ginn, T.R. (2017). Large-scale comparison of bioaugmentation and biostimulation approaches for biocementation of sands. *Journal of Geotechnical and Geoenvironmental Engineering*, 143(5), 1-13. https://doi.org/10.1061/(ASCE)GT.1943-5606.0001640.

GracePavithra, K., Jaikumar, V., Kumar, P.S., & SundarRajan, P.S. (2019). A review on cleaner strategies for chromium industrial wastewater: present research and future perspective. *Journal of Cleaner Production*, 228, 580-593. https://doi.org/10.1016/j.jclepro.2019.04.117.

Grigalavičiene, I., Rutkoviene, V., & Marozas, V. (2005). The accumlation of heavy metals Pb, Cu and Cd at roadside forest soil. *Polish Journal of Environmental Studies*, 14(1), 109-115.

He, J., Chen, X., Zhang, Q., & Achal, V. (2019). More effective immobilization of divalent lead than hexavalent chromium through carbonate mineralization by Staphylococcus epidermidis HJ2. *International Biodeterioration & Biodegradation*, 140, 67-71. https://doi.org/10.1016/j.ibiod.2019.03.012.

Hu, N., Li, Z., Huang, P., & Tao, C. (2006). Distribution and mobility of metals in agricultural soils near a copper smelter in South China. *Environmental Geochemistry and Health*, 28(1–2), 19-26. https://doi.org/10.1007/s10653-005-9007-z.

Jiang, N.J., Yoshioka, H., Yamamoto, K., & Soga, K. (2016). Ureolytic activities of a urease-producing bacterium and purified urease enzyme in the anoxic condition: implication for subseafloor sand production control by microbially induced calcite precipitation (MICP). *Ecological Engineering*, 90, 96-104. https://doi.org/10.1016/j.ecoleng.2016.01.073.

Kang, C.H., & So, J.S. (2016). Heavy metal and antibiotic resistance of ureolytic bacteria and their immobilization of heavy metals. *Ecological Engineering*, 97, 304-312. https://doi.org/10.1016/j.ecoleng.2016.10.016.

Kang, C.H., Han, S.H., Shin, Y., Oh, S.J., & So, J.S. (2014). Bioremediation of Cd by microbially induced calcite precipitation. *Applied Biochemistry and Biotechnology*, 172(6), 2907-2915. https://doi.org/10.1007/s12010-014-0737-1.

Khadim, H.J., Ammar, S.H., & Ebrahim, S.E. (2019). Biomineralization based remediation of cadmium and nickel contaminated wastewater by ureolytic bacteria isolated from barn horses soil. *Environmental Technology & Innovation*, 14, 100315. https://doi.org/10.1016/j.eti.2019.100315.

Krajewska, B. (2018). Urease-aided calcium carbonate mineralization for engineering applications: A review. *Journal of Advanced Research*, 13, 59-67. https://doi.org/10.1016/j.jare.2017.10.009.

Kumar, A., Song, H.-W., Mishra, S., Zhang, W., Zhang, Y.-L., Zhang, Q.-R, & Yu, Z.-G. (2023). Application of microbial-induced carbonate precipitation (MICP) techniques to remove heavy metal in the natural environment: a critical review. *Chemosphere*, 318, 137894. https://doi.org/10.1016/j.chemosphere.2023.137894.

Kumari, D., Pan, X., Lee, D.J., & Achal, V. (2014). Immobilization of cadmium in soil by microbially induced carbonate precipitation with Exiguobacterium undae at low temperature. *International Biodeterioration & Biodegradation*, 94, 98-102. https://doi.org/10.1016/j.ibiod.2014.07.007.

Lai, Y., Yu, J., Liu, S., Liu, J., Wang, R., & Dong, B. (2021). Experimental study to improve the mechanical properties of iron tailings sand by using MICP at low pH. *Construction & Building Materials*, 273, 121729. https://doi.org/10.1016/j.conbuildmat.2020.121729.

Landa-Marbán, D., Tveit, S., Kumar, K., & Gasda, S.E. (2021). Practical approaches to study microbially induced calcite precipitation at the field scale. *International Journal of Greenhouse Gas Control*, 106, 103256. https://doi.org/10.1016/j.ijggc.2021.103256.

Li, M., Fang, C., Kawasaki, S., Huang, M., & Achal, V. (2018). Bio-consolidation of cracks in masonry cement mortars by *Acinetobacter* sp. SC4 isolated from a karst cave. *International Biodeterioration & Biodegradation*, 141, 94-100. https://doi.org/10.1016/j.ibiod.2018.03.008.

Liu, L., Li, W., Song, W., & Guo, M. (2018). Remediation techniques for heavy metal-contaminated soils: principles and applicability. *The Science of the Total Environment*, 633, 206-219. https://doi.org/10.1016/j.scitotenv.2018.03.161.

Lyu, C., Qin, Y., Chen, T., Zhao, Z., & Liu, X. (2022). Microbial induced carbonate precipitation contributes to the fates of Cd and Se in Cd-contaminated seleniferous soils. *Journal of Hazardous Materials*, 423, 126977. https://doi.org/10.1016/j.jhazmat.2021.126977.

Maity, J.P., Chen, G.-S., Huang, Y.-H., Sun, A.-C., & Chen, C.Y. (2019). Ecofriendly heavy metal stabilization: microbial induced mineral precipitation (MIMP) and biomineralization for heavy metals within the contaminated soil by indigenous bacteria. *Geomicrobiology Journal*, 36(7), 612-623. https://doi.org/10.1080/01490451.2019.1597216.

Mitra, S., Chakraborty, A.J., Tareq, A.M., Emran, T.B., Nainu, F., Khusro, A., Idris, A.M., Khandaker, M.U., Osman, H., Alhumaydhi, F.A., & Simal-Gandara, J. (2022). Impact of heavy metals on the environment and human health: novel therapeutic insights to counter the toxicity. *Journal of King Saud University. Science*, 34(3), 101865. https://doi.org/10.1016/j.jksus.2022.101865.

Mwandira, W., Nakashima, K., & Kawasaki, S. (2017). Bioremediation of lead-contaminated mine waste by *Pararhodobacter* sp. based on the microbially induced calcium carbonate precipitation technique and its effects on strength of coarse and fine grained sand. *Ecological Engineering*, 109, 57-64. https://doi.org/10.1016/j.ecoleng.2017.09.011.

Nassar, M.K., Bastani, M., Shafei, B., Consulting, A., & Gomez, M.G. (2018). Large-scale experiments in microbially-induced calcite precipitation (MICP): reactive transport model development and prediction. *Water Resources Research*, 54(1), 480-500. https://doi.org/10.1002/2017WR021488.

Ng, W., Lee, M., & Hii, S. (2012). An overview of the factors affecting microbial-induced calcite precipitation and its potential application in soil improvement. *World Academy of Science, Engineering and Technology*, 62(2), 723-729.

Omoregie, A.I., Ouahbi, T., Basri, H.F., Ong, D.E.L., Muda, K., Ojuri, O.O., Flores, D.J., & Ammami, M.T. (2024). Heavy metal immobilisation with microbial-induced carbonate precipitation: a review. *Geotechnical Research*, 11(4), 188-212. https://doi.org/10.1680/jgere.23.00066.

Pacheco, V.L., Decol, I., & Thomé, A. (2018). Analysis of the resistance of sandy soil through the plate test after the application of the biocementation technique-Microbially Induced Calcite Precipitation. *CIATEC-UPF*, 10(2), 27-41. https://doi.org/10.5335/ciatec.v10i2.8219.

Pacheco, V.L., Bragagnolo, L., Reginatto, C., & Thomé, A. (2022). Microbially induced calcite precipitation (MICP): review from an engineering perspective. *Geotechnical and Geological Engineering*, 40(5), 2379-2396. https://doi.org/10.1007/s10706-021-02041-1.

Phillips, A.J., Gerlach, R., Lauchnor, E., Mitchell, A.C., Cunningham, A.B., & Spangler, L. (2013). Engineered applications of ureolytic biomineralization: a review. *Biofouling*, 29(6), 715-733. https://doi.org/10.1080/08927014.2013.796550.

Rajasekar, A., Wilkinson, S., & Moy, C.K.S. (2021). MICP as a potential sustainable technique to treat or entrap contaminants in the natural environment: a review. *Environmental Science and Ecotechnology*, 6, 100096. https://doi.org/10.1016/j.ese.2021.100096.

Shu, S., Zhu, W., Wang, S., Ng, W., Chen, Y., & Chiu, F. (2018). Leachate breakthrough mechanism and key pollutant indicator of municipal solid waste land fi ll barrier systems: centrifuge and numerical modeling approach. *The Science of the Total Environment*, 612, 1123-1131. https://doi.org/10.1016/j.scitotenv.2017.08.185.

Song, M., Tongyao, J., Yuan, M., Siyu, H., Li, L., & Jianguo, J. (2022). A review on the applications of microbially induced calcium carbonate precipitation in solid waste treatment and soil remediation. *Chemosphere*, 290, 133229. https://doi.org/10.1016/j.chemosphere.2021.133229.

Stocks-Fischer, S., Galinat, J.K., & Bang, S.S. (1999). Microbiological precipitation of CaCO 3. *Soil Biology & Biochemistry*, 31(11), 1563-1571. https://doi.org/10.1016/S0038-0717(99)00082-6.

Tamayo-Figueroa, D.P., Castillo, E., & Brandão, P.F.B. (2019). Metal andmetalloid immobilization by microbiologically induced carbonates precipitation. *World Journal of Microbiology & Biotechnology*, 35(4), 58. https://doi.org/10.1007/s11274-019-2626-9.

United States Environmental Protection Agency – USEPA. (1992). *Method 7196A: chromium, hexavalent (colorimetric).* Washington, D.C. Retrieved in January 26, 2023, from https://www.epa.gov/sites/default/files/2015-12/documents/7196a.pdf

United States Environmental Protection Agency – USEPA. (1996a). *Method 3050B: acid digestion of sediments, sludges, and soils*. Washington, D.C. Retrieved in January 26, 2023, from https://www.epa.gov/sites/default/files/2015-06/documents/epa-3050b.pdf

United States Environmental Protection Agency – USEPA. (1996b). *Method 3060A: alkaline digestion for hexavalent chromium.* Washington, D.C. Retrieved in January 26, 2023, from https://www.epa.gov/sites/default/files/2015-12/documents/3060a.pdf

van Paassen, L.A., Ghose, R., van der Linden, T.J.M., van der Star, W.R.L., & van Loosdrecht, M.C.M. (2010). Quantifying biomediated ground improvement by ureolysis: large-scale biogrout experiment. *Journal of Geotechnical and Geoenvironmental Engineering*, 136(12), 1721-1728. https://doi.org/10.1061/(ASCE)GT.1943-5606.0000382.

Whiffin, V.S., van Paassen, L.A., & Harkes, M.P. (2007). Microbial carbonate precipitation as a soil improvement technique. *Geomicrobiology Journal*, 24(5), 417-423. https://doi.org/10.1080/01490450701436505.

Xia, W.-Y., Feng, Y.-S., Du, Y.-J., Reddy, K.R., & Wei, M.-L. (2018). Solidification and stabilization of heavy metal-contaminated industrial site soil using KMP binder. *Journal of Materials in Civil Engineering*, 30(6), 1-9. https://doi.org/10.1061/(ASCE)MT.1943-5533.0002264.

Yang, Z., & Cheng, X. (2013). A performance study of high-strength microbial mortar produced by low pressure grouting for the reinforcement of deteriorated Masonry structures. *Construction & Building Materials*, 41, 505-515. https://doi.org/10.1016/j.conbuildmat.2012.12.055.

Yang, M., Wang, S., Liu, M., Ning, X., Wu, Y., & Nan, Z. (2023). Dose relationships and interactions of four materials and MICP technology in simultaneously reducing the exchangeable parts of As, Pb, and Cd in multiple contaminated soils. *Journal of Soils and Sediments*, 23(11), 3903-3916. https://doi.org/10.1007/s11368-023-03574-z.

Yasuhara, H., Neupane, D., Hayashi, K., & Okamura, M. (2012). Experiments and predictions of physical properties of sand cemented by enzymatically-induced carbonate precipitation. *Soil and Foundation*, 52(3), 539-549. https://doi.org/10.1016/j.sandf.2012.05.011.

Zhu, X., Li, W., Zhan, L., Huang, M., Zhang, Q., & Achal, V. (2016). The large-scale process of microbial carbonate precipitation for nickel remediation from an industrial soil. *Environmental Pollution*, 219, 149-155. https://doi.org/10.1016/j.envpol.2016.10.047.